JOURNAL OF MATERIALS SCIENCE **38** (2003) 3319–3324

Tensile behavior of bulk nanostructured and ultrafine grained aluminum alloys

B. Q. HAN, F. A. MOHAMED
Department of Chemical Engineering and Materials Science, University of California, Irvine, CA 92697-2575, USA
E-mail: famohame@uci.edu

E. J. LAVERNIA
Department of Chemical Engineering and Materials Science, University of California, Irvine, CA 92697-2575, USA; University of California, Davis, CA 95616-5294, USA

In the present study, data on tensile behavior of bulk nanostructured aluminum alloys processed via consolidation of mechanically milled powders and severe plastic deformation are analyzed. High strength and low strain hardening were observed in bulk nanostructured and ultrafine-grained Al alloys. The ductility of aluminum alloys decreases with decreasing grain size. The high amount of intercrystalline components may have an influence on tensile properties of bulk nanostructured materials when grain sizes are less than 100 nm. The high strength in bulk nanostructured Al-Mg alloy may be attributed to contributions arising from grain size strengthening, the presence of high dislocation densities, Orowan strengthening, precipitation hardening and solid-solution hardening. The large and sudden stress drops in the stress-strain curves of cryomilled Al alloys are most probably indicative of the dislocation annihilation in the vicinity of or breakaway from the strong pinning role of dispersoids.

1. Introduction

Bulk nanostructured materials (BNMs) exhibit unique microstructures [1, 2] in which the volume of grain boundary is significant. For example, a 5-nm material has approximately 50% of its volume as grain boundaries. BNMs are emerging as a new class of materials with unusual structures and, as a result, have attracted considerable attention in recent years. They offer interesting possibilities related to many structural applications.

The successful synthesis of large-scale BNMs with a grain size in the range of 10–200 nm represents a major achievement in the wide field of nanotechnology. The fact that it is now possible to synthesize large-scale BNMs with dimensions in the 10^2–10^4 mm is of technological and scientific significance. From a technological point of view, it will be feasible to obtain engineering materials that retain the structural and chemical attributes of particles in the nanometer size range. From scientific point of view, large-scale BNMs will permit careful studies of the physical and mechanical behavior, using standardized testing. In addition, BNMs, by virtue of their microstructure, will allow systematic investigations of the influence of multiple-length scales (from the nanometer to micrometer) on the fundamental physical mechanisms that govern the materials.

Severe plastic deformation (SPD) and consolidation of mechanically milled powders represent the two most widely used techniques for synthesizing bulk nanostructured aluminum alloys [2–5]. There are two main differences between these techniques in terms of the characteristics of the materials produced. First, the minimum grain size of BNMs processed via consolidation of mechanically milled powders is typically smaller than that via SPD. For instance, the minimum grain size in BNMs processed via consolidation of mechanically milled powders is about 20–30 nm (reported in a MA pure Al [6]), compared to about 100–300 nm via SPD [2]. This difference most likely is the result of: (a) the higher level of severely plastic deformation introduced during milling procedure, and (b) the limitation of grain growth by the Zener pinning of dispersoids in the former approach. Also, this difference is consistent with the general observation that the final grain size of BNMs is largely determined by the inherent thermal stability of the microstructure in combination with the parametric space used during processing [7]. Second, the tensile ductility of BNMs processed using consolidation of mechanically milled powders is lower than that of SPD, probably because of the absence of defects in the microstructure characterizing the material produced by the latter technique. As reported elsewhere [8], the low tensile ductility of many nanostructured materials is often attributed to defects and flaws.

Data reported for the mechanical behavior of bulk nanostructured aluminum alloys have shown two trends. First, for a grain size ranging from 20 to 300 nm, the grain size softening phenomenon (e.g., reverse Hall-Petch relationship [9]), which is sometimes reported, is absent, and the flow strength follows the regular Hall-Petch relationship: $\sigma = \sigma_o + k \cdot d^{-1/2}$. Second, in some BNMs [3, 10, 11], extensive strain hardening is not observed. This trend is manifested in the presence of a longer steady-stage extending from the ultimate stress to the failure point (for instance, nanostructured 5083 Al alloy [4]).

The purpose of the present study is to provide insight into the deformation behavior of bulk nanostructured aluminum alloys at ambient temperatures by close reviewing the data reported for tensile mechanical properties.

2. Tensile behavior of bulk nanostructured aluminum alloys

The comparison of tensile behavior of nanostructured aluminum alloys with coarse-grained aluminum alloys is necessary to understand the deformation mechanisms of nanostructured aluminum alloys. Fig. 1 shows the plots of true tensile stress as a function of true strain for four Al-Mg alloys, i.e., cryomilled UFG Al-7.5%Mg alloy [12], cryomilled nanostructured 5083 Al alloy [4], ultrafine-grained (UFG) 5083 Al processed via SPD (equal-channel angular pressing) [13], and as-received coarse-grained 5083 Al [13]. Cryomilled Al-7.5Mg alloy has a grain size of about 300 nm [12], and cryomilled 5083 Al alloy is reported to possess bimodal grains with some of grains of about 30 nm, and some large grains of about several hundred nanometers in microstructure after extrusion at elevated temperatures [4]. 5083 Al alloy processed via equal-channel angular pressing (ECAP) has a homogeneous uniform grain size of about 300 nm [13]. The coarse-grained 5083 Al alloy has grain sizes of 200 μm [13]. Inspection of the figure shows three observations. The first observation is related to yield strength. The yield strength of BNMs or UFG Al alloys is higher than that of coarse-grained Al alloys. The second observation is pertinent to strain hardening. The strain hardening exponent, h ($h = d \ln \sigma / d \ln \varepsilon$), is approximately 0.04 in cryomilled Al-7.5Mg alloy, about 0.07 in cryomilled 5083 Al-Mg alloy and about 0.08 in 5083 Al-Mg alloy prepared by ECAP, whereas, the strain hardening exponent is relatively high (changed from about 0.3 to about 0.1) in coarse-grained 5083 Al alloy.

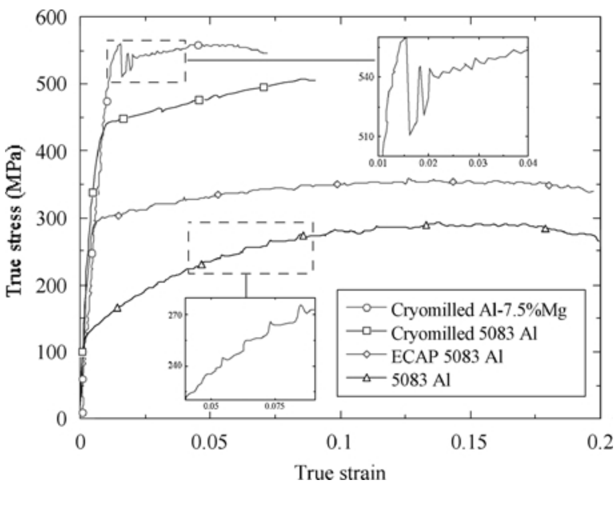

Figure 1 Plots of true tensile stress vs. true strain of Al-7.5%Mg alloy [12], 5083 Al alloy processed by consolidation of cryomilled powders [4] and 5083 Al alloy processed by equal-channel-angular pressing [13].

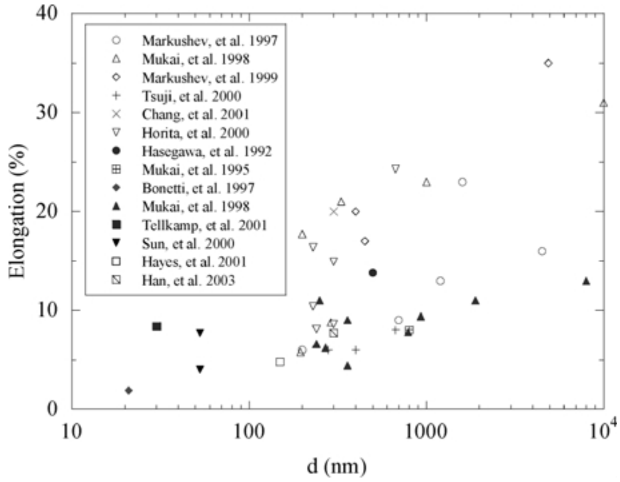

Figure 2 Tensile elongation as a function of grain size in bulk nanostructured aluminum alloys processed by consolidation of mechanically milled powders and severe plastic deformation [3–6, 11–13, 15–20].

In addition to revealing the aforementioned two observations regarding yield strength and strain hardening, the data of Fig. 1 show that cryomilled UFG Al-7.5%Mg alloy [12], cryomilled nanostructured 5083 Al alloy [4], and UFG 5083 Al alloy [13] exhibit relatively high ductilities (several to nearly 20 percent of elongation). This observation contrasts with those reported for nanostructured materials in which low tensile ductility, typically no more than 2% elongation for grain sizes less than 25 nm [14] was reported. It is noteworthy that the elongation of 5083 Al alloy processed via ECAP (20%) is essentially equal to that characterizing the as-received alloy [13].

Fig. 2 shows the tensile elongation of several aluminum alloys processed by two approaches, i.e., consolidation of mechanically milled powders and severe plastic deformation (SPD) [3–6, 11–13, 15–20] as a function of grain size. Despite considerable scatter in the data, it is seen that ductility generally decreases with decreasing grain size. Also, the trend of data appears to indicate that the processing approach has an influence on the value of elongation. For the same grain size, the values of elongation in BNMs by SPD are higher than those by consolidation of mechanically milled powders. Finally, Fig. 2 illustrates a finding that was mentioned earlier: grain refinement via SPD and consolidation of mechanically milled powders is limited to approximately 200 nm and 20 nm, respectively.

3. Discussion

3.1. Influence of intercrystalline components on mechanical properties of BNMs

When grain sizes fall in the nano-meter region (200 nm or less), the intercrystalline region, consisting of grain boundaries and triple junctions, will assume a considerable volume fraction of the overall microstructure. The grain size and grain boundary width will have a significant influence on volume fractions of intercrystalline regions in BNMs. In the analysis on the effect of grain size on volume fraction of intercrystalline region in nanocrystalline materials [21–23], the relationships among volume fractions of intercrystalline components (f_{ic}), grain boundaries (f_{gb}) and triple junctions (f_{tj}), grain size (d) and grain boundary width (w) are given by:

$$f_{ic} = 1 - (1 - w/d)^3 \tag{1}$$

$$f_{gb} = 3 \cdot (w/d) \cdot (1 - w/d)^2 \tag{2}$$

$$f_{tj} = f_{ic} - f_{gb}. \tag{3}$$

The above expressions indicate that the volume fractions of intercrystalline area, grain boundaries, and triple junctions are influenced not only by the value of grain size of the nanostructure, but also by its grain boundary width. For example, when the grain boundary width for grains with sizes of about 30 nm is assumed to be 1 nm, the volume fractions of intercrystalline regions, grain boundaries and triple junctions are about 9.67, 9.34 and 0.33 vol%, respectively.

The influence of intercrystalline regions on the overall strength in BNMs processed via SPD with the relative "larger" grain sizes might be insignificant, because of the negligible volume fraction of intercrystalline areas. By contrast, the volume fraction of intercrystalline areas in BNMs processed via consolidation of mechanically milled powders cannot be ignored, and may have a significant effect on mechanical properties, when the grain size is less than 100 nm. As grain size approaches that typical of the nanocrystalline range, microstructure can be assumed to consist of continuous grain boundaries and discontinuous grains. According to the law of mixtures, the strength (σ) of nanocrystalline materials can be expressed by [24, 25]:

$$\sigma = (1 - f_{ic}) \cdot \sigma_g + f_{ic} \cdot \sigma_{ic} \tag{4}$$

where f_{ic} is the volume fraction of intercrystalline region; σ_g and σ_{ic} are the strength in grains and the strength at intercrystalline region, respectively. From Equation 4, it may be postulated that the grain size softening (i.e., the negative Hall-Petch relation) might appear when the negative item $f_{ic} \cdot \sigma_g$ outweighs other items.

When the intercrystalline region becomes a significant fraction of the overall microstructure, the deformation mechanisms related to grain boundaries, grain boundary sliding or Coble creep, are expected to play a major role during deformation. This possibility should be investigated in future studies on BNMs.

3.2. Strengthening mechanisms

High yield and flow strength in BNMs and UFG materials can be the result of the contributions of several types of strengthening. The first contribution is from grain size strengthening. According to the Hall-Petch relation ($\sigma_d = \sigma_o + k \cdot d^{-1/2}$), there is an increase in strength with a decrease in grain size [8]. For aluminum alloys, grain size is reduced dramatically by cryomilling processing and can remain stable after subsequent consolidation by HIP treatment [5, 26]. The ultrafine grains of aluminum alloys also can be produced by severe plastic deformation [2, 13]. A second contribution to strength may be from either the presence of a high density of dislocations or the multiplication of dislocations [15]. For example, a high density of dislocations of about 1.3×10^{17} m^{-2} has been observed in cryomilled Al-7.5%Mg powders following cold pressing at 1.1 GPa [27]. However, because of the strong pinning role of dispersoids, the majority of dislocations in the consolidated cryomilled Al-7.5%Mg may be immobile. In addition, the dislocation activity in pure nanophase metals appears to decrease with decreasing grain size owing to a combination of the decreased availability of dislocations and the decreased ability to create new dislocations [28]. Consequently, dislocation strengthening may be a minor factor in cryomilled materials. Alternatively, a high density of dislocations of about 6×10^{15} m^{-2} is typically assumed in severely deformed metallic materials [2]. In addition, strong interactions of dislocations with dispersoids, i.e., Orowan strengthening, might be present in cryomilled aluminum alloys. As a result of the introduction of extraneous elements during cryomilling processing, oxide or nitride dispersoids or independent impurity elements are present in BNMs [26, 29, 30]. However, in UFG aluminum alloys processed via severe plastic deformation (equal-channel angular pressing), strong Orowan strengthening should be absent because of the lack of contamination in microstructure. Finally, in Al-Mg alloys, both solid solution and precipitation strengthening may contribute to strengthening. According to the Al-Mg phase diagram, the saturated solid solution of magnesium element in aluminum contains less than 1% magnesium [31]. The remaining magnesium in Al-Mg alloys could form precipitates of Al_3Mg_2 or $Al_{12}Mg_{17}$. In summary, the high strength in bulk nanostructured Al-Mg alloy may be attributed to contributions arising from grain size strengthening, increasing of density of dislocations, Orowan strengthening, and/or precipitation hardening and solid-solution hardening.

Theoretically, the value of Orowan strengthening can be estimated by [32, 33]:

$$\sigma_{Or} = M \frac{0.4Gb}{\pi(1-\nu)^{1/2}} \frac{\ln(\bar{d}/b)}{\bar{\lambda}} \tag{5}$$

where $M = 3.06$ is the mean orientation factor for FCC aluminum, G is the shear modulus of aluminum at room temperature, b is the Burgers vector, ν is the Poisson's ratio, $\bar{d} = \sqrt{2/3} \cdot d$ and $\bar{\lambda} = \bar{d}(\sqrt{\pi/4f} - 1)$ are the mean dispersoid size and inter-particle distance, respectively. If the mean dispersoid size and inter-particle distance were taken as 0.8 and 5.4 nm, respectively, as assumed by Tellkamp *et al.* [4], the value of Orowan stress estimated from Equation 5, using the values of G and b in reference [34], is nearly 1000 MPa. However, the above values of the mean dispersoid size and inter-particle distance appear to be not very representative since they were roughly estimated from the segregation of dispersoids along grain boundaries in the images of field-ion microscope. In addition, the distribution of overall dispersoids in the images of field-ion microscope was non-uniformly distributed. Alternatively, If the mean dispersion size in the cryomilled Al-Mg alloy is taken as 10 nm and the volume fraction of dispersoids is assumed to be 0.5% [29], the value of Orowan stress is estimated to be 123 MPa. The value of 123 MPa estimated from Equation 5 represents a significant portion of the strength difference of 160 MPa between ECAP 5083 Al, whose structure, as mentioned above, is not expected to contain dispersion particles due to the lack of contamination, and cryomilled 5083 Al. On the other hand, the strength difference of about 175 MPa between the UFG 5083 Al alloy (300 nm) processed via equal-channel-angular pressing and the coarse-grained 5083 Al alloy (200 μm) in Fig. 1 may reflect to the grain size effect, if the effect of dislocation multiplication on strengthening can be overlooked in UFG 5083 Al alloy (300 nm) processed via equal-channel-angular pressing. However, a quantitative assessment of the data of Fig. 1 in terms of the Hall-Petch equation ($\sigma_d = \sigma_o + k \cdot d^{-1/2}$) is not feasible since the value of σ_o depends on several parameters including strain and alloying elements.

3.3. Plastic deformation in tension

Examination of the plots of stress versus strain shows features that may provide insight into the details of deformation processes. According to Fig. 1, there is a short, rapid strain-hardening region in the cryomilled Al-7.5%Mg alloy, in which the multiplication of dislocations may occur. Although it is expected that strong interactions take place between dislocations and dispersoids in cryomilled Al-Mg alloys, the dislocations may be able to move after yielding. After the maximum stress, there is a rapid stress-drop and a short period of a serrated stress-strain curve. In general, there are three possible explanations for the phenomenon of serrated flow: (a) the interactions of mobile dislocations with alloying elements (dynamic strain aging), i.e., Portevin-Le Chatelier effect [35–37], (b) deformation twining [38], and (c) the detachment of dislocations from ultrafine oxide or nitride dispersoids. The first explanation appears to applicable to all the alloys partly because there are high amounts of solid solution elements and partly because the shape of serrations seem to resemble those which were reported for solid-solution alloys [35, 39, 40]. However, the characteristics of the serrations in the initial portion of the stress-strain curve of the cryomilled Al-Mg alloy are not entirely consistent with those observed in case of dynamic strain aging. In particular, demonstrated by Fig. 1, the stress drops are not only sudden but also large. On the other hand, these stress drops are similar in trend and shape to those characterizing deformation twining. Although deformation twinning was difficult in fine-grained materials despite the fact that the same material in coarse-grained form may readily yield deformation twins under similar conditions [41], deformation twins were observed in the cryomilled Al-7.5%Mg powders when examined by high-resolution TEM [42]. In addition, deformation twinning in Al-4.8%Mg alloy was also observed when it was shock loaded to 13 GPa at a temperature of −93 K, while deformation twinning in 99.99 Al and 6061 Al alloy was absent at similar conditions [43]. Gray [43] attributed the formation of deformation twins in Al-4.8%Mg to the significant role of solute strengthening, instead of the reduction of stacking fault energy. Because the supersaturated solid solution in cryomilled Al-7.5%Mg, the possibility of deformation micro-twinning in plastic deformation of cryomilled Al-7.5%Mg cannot be ruled out at the present stage. The third explanation is applicable because the pinning effect of dispersoids is much stronger than that of solute atoms. Dislocations can accumulate around ultrafine dispersoids in cryomilled Al-Mg alloy. When dislocations burst out from ultrafine dispersoids under high applied stresses or annihilate each other, a stress-drop can occur in the stress-strain curve. In summary, the dislocation annihilation in the vicinity of or breakaway from the strong pinning role of dispersoids are the mechanisms most likely to be responsible for the observed stress-drops after the yield deformation in cryomilled Al-7.5%Mg.

Tensile data on various materials suggest that the relationship between true stress, σ, and true strain, ε, is given by $\sigma = K\varepsilon^h$ [44]. If the necking occurs when $d\sigma/d\varepsilon = \sigma$ at the maximum stress, the true strain at the onset of necking (uniform strain) is given by $\varepsilon_u = h$. Consequently, the uniform strain decreases with decreasing strain-hardening exponent. An empirical relation of strain-hardening exponent and grain size (d) (less than 10 μm) in carbon steels is given by $h = 5/(10 + d^{-0.5})$ where d is in mm [45]. Accordingly, $\varepsilon_u = 5/(10 + d^{-0.5})$. When the grain sizes decrease from several hundred micrometers to several micrometers, ductility decreases with decreasing grain size [45]. Although it is not certain whether the above relationship can be applicable to materials other than carbon steels or whether can be extrapolated to the nanometer range, it at least shows the trend of the uniform strain and consequently total elongation decreasing with decreasing grain size.

It is observed that the processing approach has an influence on ductility, defined as the total elongation to failure. For example, ductility in BNMs processed by SPD is in general higher than that processed by consolidation of mechanically milled powders. According to available information, the value of uniform strain (ε_u) can be expressed as: $\varepsilon_u = \rho_m \cdot b \cdot L$ where ρ_m is the density of mobile dislocations, b the Burgers vector and L the average distance of dislocation movement. The value of total elongation is a sum of uniform strain and necking strain. As necking in BNMs is relatively small, the value of elongation can be assumed to be proportional to the density of mobile dislocations. In BNMs processed via consolidation of mechanically milled powders, most of the dislocations are highly likely to be immobilized due to their strong interactions with dispersoids. Therefore, it is expected that the density of mobile dislocations in BNMs processed via consolidation of mechanically milled powders be lower than that in materials processed via severe plastic deformation. This expectation regarding the difference in the density of mobile dislocations may explain why ductility in the former materials is lower than that in the latter materials. Another possible explanation for the lower tensile ductility of BNMs processed via consolidation of mechanically milled powders may be related to the presence of residual porosity or the presence of flaws at the interfaces of oxide particles and matrix [46]. It is well-known that even when materials consolidated under very high temperatures and high pressures, residual porosity cannot be eliminated. Finally, contamination of extraneous elements introduced during milling procedure also has a negative effect on ductility.

4. Summary
The high amount of intercrystalline components is expected to influence tensile properties of BNMs when grain sizes are less than 100 nm. The high strength in bulk nanostructured Al alloys may be attributed to contributions arising from grain size strengthening, increasing of density of dislocations, Orowan strengthening, precipitation hardening and solid-solution hardening. The dislocation annihilation in the vicinity of or breakaway from the strong pinning role of dispersoids can account for the large stress drops in the initial portion of the stress-strain curve of cryomilled Al-7.5%Mg while the occurrence dynamic strain aging appears to be responsible for the serrations in the stress-strain curves of ECAP 5083 Al and coarse–grained 5083 Al. Investigation of the occurrence of serrated flow in cryomilled Al alloys as a function of strain rate, temperature, and milling conditions should provide guiding information on the role of twinning and slip during plastic deformation (stress necessary for twinning is less sensitive to temperature than that necessary for slip). The ductility of aluminum alloys decreases with decreasing grain size. The BNMs processed via severe plastic deformation exhibit higher ductilities than those processed via consolidation of mechanically milled powders. The lower ductility in the latter materials can be the result of one or a combination of the following three possibilities: (a) the strong interaction between dislocations and dispersion particles, (b) the presence of residual porosity or the presence of flaws at the interfaces of oxide particles and matrix, and (c) the introduction of extraneous elements during milling procedures.

Acknowledgements
The work is supported by the Office of Naval Research under grant numbers N00014-01-1-0882 and N00014-03-1-0149 with Dr. Lawrence Kabacoff as program officer.

References
1. C. SURYANARAYANA, *Inter. Mater. Rev.* **40** (1995) 41.
2. R. Z. VALIEV, R. K. ISLAMGALIEV and I. V. ALEXANDROV, *Prog. Mater. Sci.* **45** (2000) 103.
3. X. K. SUN, H. T. CONG, M. SUN and M. C. YANG, *Metall. Mater. Trans.* A **31A** (2000) 1017.
4. V. L. TELLKAMP, A. MELMED and E. J. LAVERNIA, *ibid.* **32A** (2001) 2335.
5. R. W. HAYES, R. RODRIGUEZ and E. J. LAVERNIA, *Acta Mater.* **49** (2001) 4055.
6. E. BONETTI, L. PASQUINI and E. SAMPAOLESI, *NanoStruct. Mater.* **9** (1997) 611.
7. C. C. KOCH, *ibid.* **9** (1997) 13.
8. J. R. WEERTMAN, *Mater. Sci. Eng.* A **166** (1993) 161.
9. H. CONRAD and J. NARAYAN, *Scrip. Mater.* **42** (2000) 1025.
10. R. Z. VALIEV, A. V. KORZNIKOV and R. R. MULYUKOV, *Mater. Sci. Eng.* A **168** (1993) 141.
11. M. V. MARKUSHEV, C. C. BAMPTON, M. Y. MURASHKIN and D. A. HARDWICK, *ibid.* **234–236** (1997) 927.
12. B. Q. HAN, E. J. LAVERNIA and F. A. MOHAMED, *Phil. Mag. Lett.* **83** (2003) 89.
13. S. Y. CHANG, J. G. LEE, K. T. PARK and D. H. SHIN, *Mater. Trans.* **42** (2001) 1074.
14. C. C. KOCH, D. G. MORRIS, K. LU and A. INOUE, *MRS Bulletin* February (1999) 54.
15. T. HASEGAWA, T. MIURA, T. TAKAHASHI and T. YAKOU, *ISIJ Int.* **32** (1992) 902.
16. T. MUKAI, K. ISHIKAWA and K. HIGASHI, *Mater. Sci. Eng.* A **204** (1995) 12.
17. T. MUKAI, M. KAWAZOE and K. HIGASHI, *NanoStruct. Mater.* **10** (1998) 755.
18. M. V. MARKUSHEV, M. Y. MURASHKIN, P. B. PRANGNELL, A. GHOLINIA and O. A. MAIOROVA, *ibid.* **12** (1999) 839.
19. Z. HORITA, T. FUJINAMI, M. NEMOTO and T. G. LANGDON, *Metall. Mater. Trans.* A **31A** (2000) 691.
20. N. TSUJI, Y. SAITO, Y. ITO, H. UTSUNOMIYA and T. SAKAI, in "Ultrafine Grained Materials," edited by R. S. Mishra, S. L. Semiatin, C. Suryanarayana, N. N. Thadhani and T. C. Lowe (The Minerals, Metals & Materials Society, 2000) p. 207.
21. G. PALUMBO, S. J. THORPE and K. T. AUST, *Scrip. Metall. Mater.* **24** (1990) 1347.
22. N. WANG, Z. R. WANG, K. T. AUST and U. ERB, *Acta Metall. Mater.* **43** (1995) 519.
23. G. PALUMBO, K. T. AUST and U. ERB, *Mater. Sci. Forum* **225–227** (1996) 281.
24. J. E. CARSLEY, J. NING, W. W. MILLIGAN, S. A. HACKEY and E. C. AIFANTIS, *NanoStruct. Mater.* **5** (1995) 441.
25. D. A. KONSTANTINIDIS and E. C. AIFANTIS, *ibid.* **10** (1998) 1111.
26. V. L. TELLKAMP, S. DALLEK, D. CHENG and E. J. LAVERNIA, *J. Mater. Res.* **16** (2001) 938.
27. X. Z. LIAO, J. Y. HUANG, Y. T. ZHU, F. ZHOU and E. J. LAVERNIA, in "Ultrafine Grained Materials II, Seattle, WA, 2002," edited by Y. T. Zhu, T. G. Langdon, R. S. Mishra, S. L. Semiatin, M. J. Saran and T. C. Lowe (TMS, The Minerals, Metals & Materials Society) p. 323.
28. R. W. SIEGEL and G. E. FOUGERE, *NanoStruct. Mater.* **6** (1995) 205.
29. F. ZHOU, J. LEE, S. DALLEK and E. J. LAVERNIA, *J. Mater. Res.* **16** (2001) 3451.
30. O. SUSEGG, E. HELLUM, A. OLSEN and M. J. LUTON, *Phil. Mag.* A **68** (1993) 367.
31. "ASM Handbook: Alloy Phase Diagrams" (American Society for Metals, Metals Park, OH, 1992).
32. L. M. BROWN and R. K. HAM, in "Strengthening Methods in Crystals" (Elsevier, Amsterdam, 1971) p. 9.
33. B. Q. HAN and D. C. DUNAND, *Mater. Sci. Eng.* A **277** (2000) 297.
34. H. J. FROST and M. F. ASHBY, in "Deformation-Mechanism Maps: The Plasticity and Creep of Metals and Ceramics" (Pergamon Press, 1982).
35. P. LUKAC, J. BALIK and F. CHMELIK, *Mater. Sci. Eng.* A **234–236** (1997) 45.
36. P. HAHNER, *Acta Mater.* **45** (1997) 3695.
37. J. BALIK, *Mater. Sci. Eng.* A **316** (2001) 102.
38. J. W. CHRISTIAN and S. MAHAJAN, *Prog. Mater. Sci.* **39** (1995) 1.
39. F. A. MOHAMED, K. L. MURTY and T. G. LANGDON, *Acta Metall.* **22** (1974) 325.

40. J. M. ROBINSON, *Inter. Mater. Rev.* **39** (1994) 217.
41. E. EL-DANAF, S. R. KALIDINDI and R. D. DOHERTY, *Metall. Mater. Trans.* A **30A** (1999) 1223.
42. J. HE, K. H. CHUNG, X. LIAO, Y. T. ZHU and E. J. LAVERNIA, *ibid.* in press (2003).
43. G. T. GRAYIII, *Acta Metall.* **36** (1988) 1745.
44. T. H. COURTNEY, "Mechanical Behavior of Materials" (McGraw-Hill Higher Education, 2000).
45. W. B. MORRISON and R. L. MILLER, in "Ultrafine-Grain Metals" (Syracuse University Press, Syracuse, NY, 1970) p. 182.
46. M. N. RITTNER, J. R. WEERTMAN, J. A. EASTMAN, K. B. YODER and D. S. STONE, *Mater. Sci. Eng.* A **237** (1997) 185.

Received 17 April 2002
and accepted 21 May 2003